

TIME-DEPENDENT QUANTUM METHODS FOR LARGE SYSTEMS

Nancy Makri

*School of Chemical Sciences, University of Illinois, Urbana, Illinois 61801;
e-mail: nancy@makri.scs.uiuc.edu*

Key Words quantum-classical methods, mean field approximation, wavepackets, semiclassical theory, path integral, reduced density matrix, dissipation, influence functionals, system-bath models

■ **Abstract** This review focuses on time-dependent methods suitable for simulating the quantum dynamics of processes in large clusters and condensed-phase environments. A number of mean field, quantum-classical, and quantum statistical approximations that avoid the conventional exponential scaling with the number of degrees of freedom are reviewed. In addition, rigorous semiclassical and path integral approaches are described that are feasible in certain physical situations. Select chemical applications illustrating the capabilities of these methods are discussed.

INTRODUCTION

The past two decades have witnessed an explosion in the development of theoretical schemes for simulating the dynamics of molecular systems. Motivated by major advances in time-resolved spectroscopic techniques and catalyzed by the availability of powerful computational resources, numerical simulations allowed for the first time a glimpse into the course of fundamental chemical processes and the microscopic changes that accompany the transformation of reactants to products. Perhaps the most useful and widespread of these schemes continues to be the molecular dynamics (MD) method, which integrates the classical equations of motion. Because of its simplicity, MD is routinely applicable to systems of thousands of atoms. In addition, interpretation of the MD output is straightforward and allows direct visualization of a process. The major shortcoming of the MD approach is its complete neglect of quantum mechanical effects, which are ubiquitous in chemistry: The majority of chemical or biological processes of interest involve the transfer of at least one proton or electron, which exhibits large tunneling or nonadiabatic effects; water, the most common solvent, is organized into a complex network of hydrogen bonds whose continuous rearrangement is inherently a quantum mechanical phenomenon; and zero-point motion constrains the energy available in a chemical bond to be smaller than that predicted by the

potential depth, and thus, MD calculations often result in spurious dissociation events.

Significant efforts in the field of chemical dynamics have been devoted to the development of quantum mechanical methods. Because of the delocalized nature of quantum mechanics, full representation of the wavefunction on a grid or basis set requires effort that grows exponentially with the number of interacting degrees of freedom. This scaling is the major stumbling block that restricts, in practice, full solution of the Schrödinger equation to small systems. Furthermore, apart from storing the wavefunction, integration of the Schrödinger equation requires application of the Hamiltonian or the time-evolution operator, and these procedures scale worse than linearly with the number of grid points or basis functions employed. Finally, the simulation of processes described by mixed ensembles, such as thermally averaged rate coefficients or correlation functions, requires propagation of a density matrix whose size is equivalent to the square of that required for storage of a wavefunction.

A number of efficient methods are now available for numerically exact wavefunction propagation in systems of a few degrees of freedom. These methods, which generally use spectral representations or polynomial expansions of the time evolution operator, have been reviewed extensively and are not elaborated in this article. Calculations in large polyatomic systems require the use of various approximations, which in a broad sense are built around mixed quantum-classical, variational, semiclassical, or path integral ideas. An exception is a class of condensed-phase processes involving a particle in a dissipative bath of phonons, whose dynamics can now be followed within numerically exact calculations.

This review focuses on time-dependent methods that are applicable to processes in large clusters and condensed phases, described by nonrelativistic Hamiltonians of distinguishable particles. Methods that scale exponentially with system size are not discussed, even though numerical applications on polyatomic molecules may have been reported. Furthermore, it focuses on strictly numerical schemes requiring large-scale computation and refrains from discussing elegant theoretical treatments that are primarily analytic in nature, such as advances in the correlation function formalism of reaction rates and molecular spectroscopy, instanton methods, or the Redfield approach. The goal is to offer the reader the general ideas underlying available methods and their range of application, rather than an exhaustive review of the literature. For this reason, only selected references are cited, which can serve as a starting point for further study.

A few words about terminology and classification of the various methods are also in order. The various schemes reviewed are grouped in sections according to the type of idea on which they are based. The term semiclassical is used to indicate the rigorous theory based on the asymptotic $\hbar \rightarrow 0$ limit of quantum mechanics and does not include other approximations that are intermediate in spirit between quantum and classical formulations.

The next section discusses the time-dependent self-consistent field method and its various extensions. The section following that focuses on hybrid quantum-

classical, Gaussian wavepacket, and surface hopping schemes. A number of appealing semiclassical ideas are next reviewed, followed by discussion of path integral methods and their application to condensed-phase dynamics and finally some concluding remarks.

TIME-DEPENDENT SELF-CONSISTENT FIELD METHODS

The time-dependent self-consistent field (TDSCF) approximation arises from time-dependent variational principles (1, 2) if the latter are applied to a product wavefunction. For a system of n degrees of freedom described by the coordinates x_i , the TDSCF ansatz for the wavefunction at a time t is

$$\Psi_{\text{TDSCF}}(x_1, \dots, x_n; t) = e^{i\varphi(t)} \prod_{i=1}^n \psi_i(x_i; t), \quad 1.$$

where $\varphi(t)$ is an insignificant phase. The evolution of the single-particle functions ψ_i is easily determined by substituting Equation 1 in the time-dependent Schrödinger equation and projecting on each of these functions. The result is (1, 3–7)

$$i\hbar \frac{\partial \psi_i(x_i, t)}{\partial t} = \prod_{j \neq i}^n \langle \psi_j(t) | H | \psi_j(t) \rangle \psi_i(t). \quad 2.$$

For Cartesian Hamiltonians, in which the kinetic energy operator is separable, the last equation can be rewritten in the form

$$i\hbar \frac{\partial \psi_i(x_i, t)}{\partial t} = -\frac{\hbar^2}{2m_i} \frac{\partial^2}{\partial x_i^2} \psi_i(x_i; t) + V_i^{\text{av}}(x_i; t) \psi_i(x_i; t), \quad 3a.$$

where

$$V_i^{\text{av}}(x_i; t) = \prod_{j \neq i}^n \langle \psi_j(t) | V | \psi_j(t) \rangle. \quad 3b.$$

According to the last equation, the evolution of each single-particle wavefunction is governed by an effective one-dimensional Schrödinger equation that involves the average potential with respect to all other degrees of freedom. Thus, Equation 2 is a mean field approximation. Its main attraction is the apparent reduction of computational effort for solving the full n -dimensional problem to that required to integrate n one-dimensional ones. In actual calculations, however, determination of the effective mean field potential requires multidimensional integration and thus is not practical for polyatomic systems unless the potential itself can be approximated by low-order polynomial expansions. The TDSCF scheme can be shown to conserve the norm of the wavefunction and the total energy. Note that the TDSCF equations are nonlinear, and thus the accuracy of the method depends on the choice of coordinate system as well as the initial condition. Rom

et al (8) concluded that normal mode coordinates are optimal for systems that do not undergo substantial structural isomerization; this is so because the normal coordinate transformation eliminates potential couplings through quadratic order.

The so-called classical separable potential (CSP) method (9) aims at enhancing the practicality of the TDSCF approximation by eliminating the expensive averaging of the multidimensional potential. According to the CSP scheme, the initial wavefunction is transformed to the Wigner phase-space representation (10), which is used to generate the weights w_α of coordinates $x_j^{(\alpha)}$ and momenta $p_j^{(\alpha)}$ that serve as initial conditions for classical trajectories. The latter are used to construct a time-dependent CSP according to the prescription

$$V_j^{\text{CSP}}(x_j; t) = \sum_{\alpha=1}^M w_\alpha V(x_1^{(\alpha)}(t), \dots, x_{j-1}^{(\alpha)}(t), x_j, x_{j+1}^{(\alpha)}(t), \dots, x_n^{(\alpha)}(t)) + \frac{1-n}{n} \bar{V}(t), \quad 4.$$

where M is the number of sampled trajectories and $\bar{V}(t)$ is the potential average with respect to the given time-evolved distribution. The CSP potential is then used to propagate the wavefunction of each mode separately. Although self consistency is no longer satisfied, causing lack of strict energy conservation, test calculations have shown that for moderately quantum mechanical systems and relatively short time periods, the CSP method gives results in quantitative agreement with full TDSCF while reducing enormously the computational effort required (11, 12).

By virtue of the time-dependent effective potential terms, the TDSCF equations allow energy flow among the various modes. This effect is illustrated nicely in simulations of the photodissociation of van der Waals clusters (5, 13, 14) and also in studies of the transition-state dynamics of ClHCl^- (15). Recent calculations of argon scattering from a cluster of 11 water molecules (16) revealed the importance of quantum effects in low-energy collisions, which are adequately captured by the TDSCF approximation as long as structural rearrangements of the cluster are not large. Specifically, the quantum TDSCF treatment resulted in appreciable energy transfer only into the softest vibrational modes of the cluster, whereas a classical MD treatment allowed excitation of modes corresponding to a wide range of frequencies.

On the other hand, dynamical correlations are completely neglected in TDSCF, implying the method can break down if the true wavefunction has a strong non-product character. Indeed, TDSCF fails to describe important phenomena, such as wavepacket splitting, that are ubiquitous in chemistry. This is because the averaging inherent in the TDSCF approach completely wipes out important features of the potential. Consider, for example, tunneling in a double-well potential coupled bilinearly to an oscillator (see Figure 1). If the initial wavefunction is centered around one of the stable minima, the mean force of the oscillator results in a TDSCF Schrödinger equation with a skewed effective potential for the tunneling

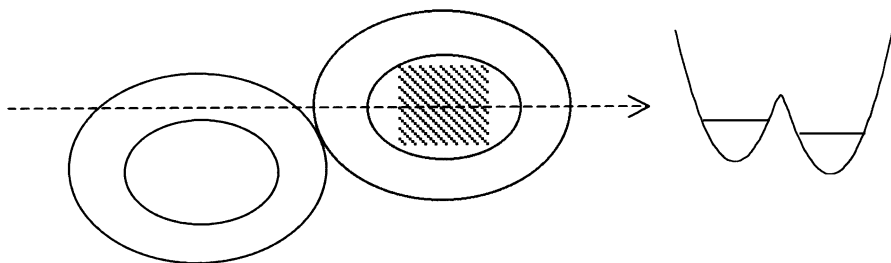


Figure 1 Contour sketch of a symmetric double-well potential and the effective one-dimensional mean field potential corresponding to a wavefunction that is localized about the right minimum. The shaded region indicates the wavefunction. The asymmetry of the effective mean field potential prevents tunneling.

coordinate, and thus (unless the coupling forces are extremely small) tunneling is blocked (17).

A number of approaches have been introduced in order to amend the shortcomings of TDSCF. Perhaps the simplest improvement is to add important two-body correlations explicitly (18). The most systematic remedy is the inclusion of multiple product-type configurations. The multiconfigurational extension (MC-TDSCF) (17, 19) expands the wavefunction as follows:

$$\Psi_{\text{MC-TDSCF}}(x_1, \dots, x_n; t) = \sum_{\alpha_1} \cdots \sum_{\alpha_L} c_{\alpha_1, \dots, \alpha_L}(t) \prod_{k=1}^n \psi_{\alpha_k}(x_k; t), \quad 5.$$

where L is the total number of configurations. The expansion coefficients are given by differential equations, which are solved self-consistently with the single-mode wavefunctions. The appeal of this idea is that even a small number of configurations can lead to physically meaningful results, although the ability to identify those important configurations rests solely on one's insight into a particular problem. In the limit where the number of configurations becomes large, the MC-TDSCF scheme reverts to a full basis set expansion and is accompanied by the conventional exponential scaling, although generally with a smaller exponent (20). With a moderate number of configurations, MC-TDSCF leads to semiquantitative results for systems with several atoms while retaining practicality. Typical applications of the method include the study of the dissociation dynamics of NO_2 (21) and the absorption spectrum of pyrazine in a model environment of 24 harmonic vibrational modes (22).

Another, perhaps simpler, possibility is the configuration interaction version (CI-TDSCF) (23, 24), which optimizes variationally the coefficients in an expansion of the type

$$\Psi_{\text{CI-TDSCF}}(x_1, \dots, x_n; t) = \sum_{\alpha=1}^L a_{\alpha}(t) \prod_{k=1}^n \psi_k(x_k; t). \quad 6.$$

In this sense, the TDSCF ansatz is used here only as a physically meaningful basis set, and thus the CI-TDSCF scheme converges to the exact results in the $L \rightarrow \infty$ limit.

Finally, note that with proper adjustment, the TDSCF scheme can be cast into a form suitable for ensemble averaged quantities (25–27); however, the latter is practical only if the majority of degrees of freedom (those of the bath) are harmonic.

MIXED QUANTUM-CLASSICAL METHODS

The idea of treating select degrees of freedom in a polyatomic system quantum mechanically while retaining a classical trajectory description for those degrees of freedom that surround the coordinate of interest dates back to the first attempts to describe the dynamics of complex chemical systems. The appeal of hybrid quantum-classical (QC) schemes is that tunneling or interference phenomena that may be important for one or two reaction coordinates can be fully accounted for while—by treating the remaining degrees of freedom classically—conventional exponential scaling is avoided. Unfortunately, no rigorous ways of mixing quantum and classical mechanics are known, and several hybrid schemes retain a strong mean field flavor.

A variety of mixed QC approximations can be derived from the TDSCF equations. Consider, for example, a Hamiltonian where the reaction coordinate s is described quantum mechanically and the solvent coordinates \mathbf{x} are treated via classical mechanics. Unfortunately, the structure of quantum mechanics is different from the classical mechanical formalism, and describing the dynamics between classical and quantum variables is not easy. Once the mean field factorization is imposed, one can imagine propagating the wavefunction ψ_0 for the quantum particle according to a Schrödinger equation in which the mean potential interaction due to the solvent is computed in terms of classical trajectories (1, 28):

$$i\hbar \frac{\partial \psi_0(s; t)}{\partial t} = -\frac{\hbar^2}{2m_0} \frac{\partial^2}{\partial s^2} \psi_0(s; t) + V_0^{\text{av}}(s; t) \psi_0(s; t). \quad 7.$$

At the same time, each classical variable is subjected to a quantum force that is calculated as the expectation value with respect to the wavefunction of the system.

$$\dot{x}_i(t) = \frac{p_i(t)}{m_i}, \quad \dot{p}_i(t) = -\left\langle \psi_0(t) \left| \frac{\partial V}{\partial x_i} \right| \psi_0(t) \right\rangle. \quad 8.$$

The initial conditions for these trajectories can be selected according to a Wigner prescription (10) or, in cases of locally integrable dynamics, from an action-angle variable transformation (29).

Although the above equations are intuitively appealing, their interpretation and numerical implementation is not unique. Perhaps the strictest interpretation is to use in Equation 7 the average of the potential with respect to all solvent trajectories at a given time (5, 30, 31). This idea, sometimes referred to as the self-consistent

trajectory bundle, closest in spirit to the mean field approach, is plagued by problems similar to those of the fully quantum version of TDSCF. Namely, too much averaging is performed, and essential features of the potential are lost. An attractive alternative is a local QC scheme where the solvent potential felt by the quantum degree of freedom is given by a single trajectory (32). This version, which also follows from Ehrenfest's theorem (33), retains local aspects of the potential and thus generally performs considerably better, at the cost of solving a separate Schrödinger equation for each propagated classical trajectory. Numerical tests on a double well coupled to a thermal bath of harmonic oscillators indicate that the local QC TDSCF can be almost quantitative in describing the tunneling dynamics of an initially localized state when the overall coupling strength is not very large (34). Other recent work has shown that significant discrepancies can still arise in the estimation of rate constants, especially at moderate-to-strong system-bath couplings (35). Given that the equations are nonlinear, the significant differences in the conclusions reached by these works are likely to originate from their use of different initial conditions. Nevertheless, QC methods are inherently inadequate for calculating quantities that are sensitive to phase factors and time-dependent wavefunction overlaps. For example, they fail even qualitatively to yield the absorption cross section, as the latter is determined by the autocorrelation function of the nuclear coordinates, which is missing from the QC treatment (31, 36). Furthermore, recent studies of coupled oscillator models have shown that mixed QC treatments can in some situations be less satisfactory than a classical treatment of all modes (37–39).

Mixed QC ideas are also relevant in the treatment of nonadiabatic processes in large molecules or the condensed phase. Even if the MD method is adequate for the purpose of describing the dynamics on a single Born-Oppenheimer potential surface, it does not allow for a change of electronic state. The mixed QC schemes described above can be extended to deal with electronic nonadiabaticity (40, 41). Problems may arise because the average force that drives the nuclear motion can be vastly different from the true force that should govern the time evolution on each individual potential surface. The averaging inherent to these methods can lead to unphysical results, as the wavepacket may exit the nonadiabatic region experiencing an average potential rather than the true Bohn-Oppenheimer potential of a given electronic state (43). An elegant extension of the Ehrenfest model that properly incorporates boundary conditions specific to the electronic states of interest is the classical electron model of Meyer & Miller (42).

Electronically nonadiabatic effects can be included in trajectory simulations according to a number of ad hoc procedures generally known as surface-hopping methods. In the original scheme of Tully & Preston (44), a swarm of classical trajectories with initial conditions selected to represent the desirable state are propagated on a single electronic surface until an avoided surface crossing is reached. At such points, the trajectory swarm is split into two branches, each of which follows a different potential surface. Each hopping event amounts to adjusting the velocity with a hopping probability, which is given by the semiclassical Landau-Zener formula (45–47). The method has been generalized to allow hops

at any time according to a “fewest-switches” algorithm (43). This way, the need to know the location and geometry of the avoided crossing regions is avoided. The hopping probability is estimated from amplitudes obtained by solving the electronic Schrödinger equation self-consistently with the classical mechanical equations of motion. If a switch occurs, the component of velocity in the direction of the nonadiabatic coupling vector is adjusted to conserve the total energy. The surface-hopping method is practical for large systems, and several applications to nonadiabatic dynamics of molecule-surface collisions and excess electrons in atomic fluids (48) have been presented.

The ideas of surface hopping have been extended to treat processes associated with quantum mechanical transitions of a light particle (e.g. a proton) on a single electronic potential surface (49). The heavy atoms are described by classical trajectories that evolve on vibrationally adiabatic potential surfaces associated with the quantum particle, and transitions between these surfaces are treated as hopping events. The method has been applied to complex chemical processes, such as the dynamics of proton transfer in liquid methyl chloride (49). Extensions to a multiconfigurational scheme have been formulated (50, 51), and applications to proton transfer along water chains have been reported (51). These calculations indicate that fluctuating electric fields and structural constraints strongly affect the dynamics of proton transport in biological water channels.

Three decades ago, Pechukas formulated a rigorous self-consistent trajectory treatment of nonadiabatic dynamics (52). In this theory, the quantum system influences the classical dynamics via a quantum force. In turn, the quantum force on the classical degrees of freedom is obtained self-consistently with the classical trajectory. As a consequence, the force required to solve Newton’s equations is not known a priori, and thus the implementation of Pechukas’ elegant theory is not easy. Recent theoretical efforts have discussed the close connections of the surface-hopping method with this rigorous semiclassical approach (53).

Another way of accounting for electronic transitions in condensed-phase MD simulations has also been motivated by the semiclassical nonadiabatic theory of Pechukas. In this stochastic version of surface hopping, a hopping probability is constructed from the nonadiabatic transition amplitude corresponding to a particular time interval over which coherent propagation is implemented (54). This time length is not understood as a convergence parameter but rather must be chosen on the order of the decoherence time characterizing the process of interest. Coherence is dropped for times longer than that time interval. Stochastic surface hopping reverts to Tully’s method (43) in the limit of very small decoherence time intervals. In the limit of very small decoherence time intervals, Webster et al (55) used the method to study the solvation dynamics of an electron injected into a simulation box comprising 200 water molecules at equilibrium in an attempt to explain the two-phase time evolution of the experimental transient absorption spectrum of the hydrated electron (56). The calculations revealed the formation of a relatively long-lived solvated excited state of approximate *p*-type symmetry, in qualitative agreement with the experimental findings. Recent efforts have resulted in schemes

that combine the fewest-switches surface-hopping approach with a mean field force (57).

A fundamental problem common to methods that treat only some degrees of freedom quantum mechanically while resorting to classical descriptions for the remaining particles is their inability to guarantee the correct equilibrium distribution over long time periods. The origin of this flaw is the fundamental incompatibility of quantum and classical mechanical laws and characterizes even the most rigorous QC methods.

A conceptually different approach is the Gaussian wavepacket (GWP) propagation method pioneered by Heller (58). This is based on the ansatz that a Gaussian initial state remains Gaussian during the course of evolution:

$$\Psi(\mathbf{x}; t) = \exp\left(\frac{i}{\hbar}(\mathbf{x} - \mathbf{x}_t) \cdot \boldsymbol{\alpha}_t \cdot (\mathbf{x} - \mathbf{x}_t) + \frac{i}{\hbar}\mathbf{p}_t \cdot (\mathbf{x} - \mathbf{x}_t) + \frac{i}{\hbar}\gamma_t\right). \quad 9.$$

Subject to this constraint, Heller (58) obtained equations of motion for the center, width, and phase of the wavepacket. Specifically, the center \mathbf{x}_t and mean momentum \mathbf{p}_t of the wavepacket follows the classical equations of motion in the full Hamiltonian, whereas the remaining parameters are specified by the locally quadratic time-dependent harmonic approximation to the potential around the given classical trajectory. In this sense, the GWP “dresses” a classical trajectory, introducing quantum effects in an otherwise classical MD calculation. Even more practical is the frozen Gaussian approximation (59), in which the width of the wavepacket is fixed during evolution.

The above remarks suggest that the GWP method should be adequate for studying photodissociation or radiationless transitions in some polyatomic systems. Such processes are often characterized by broad and structureless spectra, implying that the dynamics must be followed for short time intervals. Vibrational structure is associated with recurrences in the correlation function, which are captured correctly as long as they originate from the harmonic part of the potential. Early applications of the method on the photodissociation of CH_3I and of ICN demonstrated the feasibility and potential accuracy of the method for such “direct” dynamical processes (60, 61).

The GWP ansatz is exact for quadratic Hamiltonians. When anharmonic problems are considered, the major shortcomings of GWP methods arise from the localized nature of the Gaussian assumption: Splitting is prohibited, and as a result, dynamical effects in considerably anharmonic systems are described properly only over short time intervals. Classically forbidden regions are penetrated only by the tail of the wavepacket. In addition, the average energy of the wavepacket is not conserved because the underlying locally harmonic potential is time dependent. Improved descriptions are achieved by employing a set of frozen Gaussians as a time-dependent basis set in terms of which the wavefunction of interest or the propagator is expanded at select time intervals (62, 63). Unfortunately, as with any basis set method, the numerical effort involved grows exponentially with the number of coupled degrees of freedom. However, if the single Gaussian approximation

already provides a physically meaningful description for a given problem, it is likely that adequate results can be obtained with a small number of such basis functions.

Another method in the spirit of QC ideas is the multiple spawning method for nonadiabatic dynamics (64, 65). The nuclear wavefunction associated with each electronic state is represented as a linear combination of multidimensional frozen Gaussian basis functions whose centers follow the classical equations of motion. Whenever a basis function enters a region of significant nonadiabatic coupling, additional basis functions are spawned in the new electronic state and evolve according to amplitudes obtained from the time-dependent Schrödinger equation. Deletion of linearly dependent functions prevents the basis from growing too large. The method has been shown to provide an accurate description of model nonadiabatic events in two spatial dimensions (66). Approximation of the wavefunction of each electronic state by a single traveling Gaussian makes the method practical for multidimensional systems, and application to studies of electronic quenching in polyatomic molecules (64, 67) and to the *cis-trans* isomerization of bacteriorhodopsin (68) have been reported.

SEMICLASSICAL METHODS

Semiclassical theory was developed in the early days of quantum mechanics as a means of merging the gap between the new theory and the established classical laws. The WKB method and its time-dependent analog, the semiclassical propagator, offer a sufficiently satisfactory connection in the small \hbar regime. The semiclassical approximation to the propagator can be obtained directly as the stationary-phase limit of the path integral and takes the form (69)

$$\langle \mathbf{x}_f | e^{-iHt/\hbar} | \mathbf{x}_0 \rangle_{\text{SC}} = \sum_{\substack{\text{all classical paths } \mathbf{x}_{\text{cl}} \\ \text{with } \mathbf{x}_{\text{cl}}(0)=\mathbf{x}_0, \mathbf{x}_{\text{cl}}(t)=\mathbf{x}_f}} (2\pi\hbar)^{-\frac{n}{2}} \det \left(\frac{\partial^2 S}{\partial \mathbf{x}_0 \partial \mathbf{x}_f} \right)^{\frac{1}{2}} e^{iS[\mathbf{x}_{\text{cl}}]/\hbar} e^{-i\mu\pi/2}.$$

10.

Here S is the classical action and μ is the Maslov phase, which (for standard Cartesian Hamiltonians) increments by unity every time the trajectory encounters a focal point or caustic. Note that in this endpoint formulation there can be multiple classical trajectories satisfying the appropriate boundary conditions. Equation 10 was first obtained by Van Vleck (69). As the stationary-phase limit of the path integral expression, it is exact for quadratic Hamiltonians. It is capable of describing semiquantitatively important quantum phenomena, (29, 70, 71). Furthermore, the semiclassical propagator has been shown to be highly accurate in nontrivial situations (72), including two-dimensional chaotic systems, thereby providing a very desirable alternative to full quantum dynamics for many-body problems.

However, numerical implementation of time-dependent semiclassical theory has in the past been problematic. One of the major drawbacks of the Van Vleck expression is that the relevant trajectories must satisfy double-ended boundary value conditions. An attractive alternative is offered by Miller's initial value representation of the survival amplitude or similar correlation functions (73). In this, one changes the integration variable associated with the propagator endpoint to an initial momentum, bringing the expression in the form of an integral over phase-space variables that specify the trajectory initial conditions:

$$\begin{aligned}
 \langle \Psi(0) | \Psi(t) \rangle &= \int d\mathbf{x}_0 \int d\mathbf{x}_f \Psi_0(\mathbf{x}_0) \Psi_0^*(\mathbf{x}_f) \\
 &\times \sum_{\substack{\text{classical paths } \mathbf{x}_{cl} \\ \text{with } \mathbf{x}_{cl}(0)=\mathbf{x}_0, \mathbf{x}_{cl}(t)=\mathbf{x}_f}} (2\pi\hbar)^{-\frac{n}{2}} \det\left(\frac{\partial^2 S}{\partial \mathbf{x}_0 \partial \mathbf{x}_f}\right) e^{iS[\mathbf{x}_{cl}]/\hbar} e^{-i\mu\pi/2} \\
 &= \int d\mathbf{x}_0 \int d\mathbf{p}_0 \Psi_0(\mathbf{x}_0) \Psi_0^*(\mathbf{x}_f) (2\pi\hbar)^{-\frac{n}{2}} \det\left(\frac{\partial \mathbf{x}_f}{\partial \mathbf{p}_0}\right)^{\frac{1}{2}} e^{iS[\mathbf{x}_{cl}]/\hbar} e^{-i\mu\pi/2}.
 \end{aligned}
 \tag{11}$$

Note that the sum over multiple paths has been absorbed in the integral over initial conditions. Apart from eliminating the cumbersome root search, another attractive feature of Equation 11 is that the divergence associated with caustics has been eliminated, as the zeros of the prefactor now appear in the numerator. From the numerical standpoint, an attractive representation is in terms of coherent states. Herman & Kluk (74) have shown that the semiclassical propagator can be expressed in the form

$$\begin{aligned}
 \langle \mathbf{x}_2 | e^{-iHt/\hbar} | \mathbf{x}_1 \rangle &= (2\pi\hbar)^{-n} \int d\mathbf{x}_0 \int d\mathbf{p}_0 D(\mathbf{x}_0, \mathbf{p}_0) e^{iS(\mathbf{x}_0, \mathbf{p}_0)/\hbar} \\
 &\times \langle \mathbf{x}_2 | G(\mathbf{x}_f, \mathbf{p}_f) \rangle \langle G(\mathbf{x}_0, \mathbf{p}_0) | \mathbf{x}_1 \rangle.
 \end{aligned}
 \tag{12}$$

Here $\mathbf{x}_f, \mathbf{p}_f$ are the endpoints of a classical trajectory with initial conditions $\mathbf{x}_0, \mathbf{p}_0$.

$$D(\mathbf{x}_0, \mathbf{p}_0) = \det \left[\frac{1}{2} \left(\frac{\partial \mathbf{x}_f}{\partial \mathbf{x}_0} + \frac{\partial \mathbf{p}_f}{\partial \mathbf{p}_0} - 2i\hbar \frac{\partial \mathbf{x}_f}{\partial \mathbf{p}_0} \cdot \boldsymbol{\gamma} + \frac{i}{2\hbar} \boldsymbol{\gamma}^{-1} \cdot \frac{\partial \mathbf{p}_f}{\partial \mathbf{x}_0} \right) \right]^{\frac{1}{2}} \tag{13}$$

is the appropriate prefactor, and the coherent state wavefunctions are

$$\langle \mathbf{x} | G(\mathbf{x}_0, \mathbf{p}_0) \rangle = \det \left(\frac{2\boldsymbol{\gamma}}{\pi} \right)^{\frac{1}{2}} \exp \left(-(\mathbf{x} - \mathbf{x}_0) \cdot \boldsymbol{\gamma} \cdot (\mathbf{x} - \mathbf{x}_0) + \frac{i}{\hbar} \mathbf{p}_0 \cdot (\mathbf{x} - \mathbf{x}_0) \right). \tag{14}$$

Another convenient form is the cellular representation by Heller (75), which employs Gaussian basis sets. A mixed treatment, employing the coherent state representation for the most important degrees of freedom while retaining a GWP description of the remaining coordinates, has been found useful and applied to diatomics in rare gas hosts (76, 77). A combination of the coherent state representation and the cellular dynamics approach has also been proposed (78).

Given the above numerically advantageous representations, the remaining problem is the highly oscillatory structure of the semiclassical propagator, which obviates the use of importance sampling procedures and thus limits applications to low-dimensional problems. Grossmann (79) discussed the technical issues in detail. To circumvent the phase cancellation problem, Walton & Manolopoulos (78) have resorted to a filtering procedure in the spirit of stationary-phase smoothing techniques developed earlier for the real time path integral (80, 81). Using this approach, Brewer et al (82) recently reported semiclassical calculations of the photodetachment spectrum of a negatively charged argon-iodine cluster treating explicitly up to 15 vibrational degrees of freedom.

In order to describe ensemble-averaged correlation functions or density matrices, one needs to square the time-dependent amplitude prior to performing the necessary trace operation. This procedure results in expressions that involve two time-evolution operators, one of which can be interpreted as a backward propagation step. The presence of two propagators leads to a double phase-space integral, increasing further the difficulty of the calculation. Sun & Miller (83) introduced a linearization approximation in which the phase of the integrand is expanded through linear terms in the difference of these integration variables, and one of these phase-space integrals is performed analytically. The result, also obtained by Pollak & Liao in the context of quantum transition state theory (84), is an appealing expression that involves the product of Wigner functions for the initial density evaluated at the initial and final phase-space values of each sampled classical trajectory. Phase oscillation is no longer problematic, making the method easily applicable to polyatomic problems. Model calculations have shown the linearized approximation to be successful for describing quantum dynamics at short time intervals, including interference phenomena (85). Nevertheless, quantum effects enter only via the Wigner functions of the initial and final states, and the real time dynamics are treated in a purely classical fashion. For this reason, the linearized semiclassical approximation cannot describe quantum interference phenomena associated with long-time recurrences (86).

Makri & Thompson (87–89) have pointed out that it is possible to exploit the structure of ensemble-averaged correlation functions or expectation values in order to alleviate the severe phase cancellation without introducing uncontrolled approximations. The key idea is that the forward and reverse time-evolution operators for the degrees of freedom that are not probed in a calculation can be combined in a single operator and evaluated semiclassically. The advantage is that the backward propagation results in considerable cancellation, and the resulting accumulated

action is small on the scale of Planck's constant, such that the integrand is smooth. Consider, for example, a correlation function of the type

$$C(t) = \text{Tr}(\rho(0) A e^{iHt/\hbar} B e^{-iHt/\hbar}), \quad 15.$$

where $\rho(0)$ is the density operator of the initial ensemble and A and B are operators that depend only on the position s of the observable system whose conjugate momentum is denoted as p . The remaining n degrees of freedom not probed in the calculation (the solvent) are denoted collectively by the canonically conjugate variables represented by the n -dimensional vectors \mathbf{R} and \mathbf{P} . One can show that using the semiclassical approximation, Equation 15 can be brought in the form (89)

$$C(t) = \int ds_0 \int ds_t \int ds_f \int d\mathbf{R}_0 \int d\mathbf{R}_f A(s_f) B(s_0) \langle s_0 \mathbf{R}_0 | \rho(0) | s_f \mathbf{R}_f \rangle \\ \times \sum_{\substack{\text{forward system} \\ \text{paths } s_{\text{cl}}^+}} \sum_{\substack{\text{backward system} \\ \text{paths } s_{\text{cl}}^-}} \sum_{\substack{\text{forward-backward} \\ \text{solvent paths } \mathbf{R}_{\text{cl}}}} D \exp\left(\frac{i}{\hbar} S_{\text{for-back}}[s_{\text{cl}}^+, s_{\text{cl}}^-, \mathbf{R}_{\text{cl}}]\right). \quad 16.$$

Here $s_{\text{cl}}^+(t')$ and $s_{\text{cl}}^-(t')$ are the system components of classical trajectories in the forward and backward time direction, with phase-space endpoints $(s_0 p_0, s_t p'_t)$ and $(s_t p_t, s_f p_f)$, respectively; \mathbf{R}_{cl} is the solvent component of these trajectories along the entire forward-backward contour; and $S_{\text{for-back}}$ is the corresponding action functional. Note that the solvent trajectory is continuous at the time t , whereas the presence of the operators in Equation 15 introduces a discontinuity in the system component of the forward-backward paths. Miller has arrived at slightly different versions by writing the system operators in exponential form according to Weyl transformations (90). The fact that the forward and backward propagation steps are combined for the majority of degrees of freedom leads to action integrals that are small, thus dramatically reducing the oscillatory character of the integrand. In essence, the major advantage of the forward-backward semiclassical dynamics (FBSD) approach is that the bulk of the cancellation occurs in the action rather than via the rapid oscillations of the integrand. As a result, Monte Carlo evaluation is easily feasible. Equation 16 can be expressed in the coherent state representation in which the integration variables are the initial positions and momenta (89).

PATH INTEGRAL METHODS

Feynman's path integral formulation of time-dependent quantum mechanics (91) provides, at least in principle, an attractive alternative to the Schrödinger approach. By representing the quantum mechanical propagator as a sum over paths, the path

integral avoids the storage problems of the wavefunction description. However, even for small systems, explicit summation requires astronomical numbers of paths, and the latter proliferate at exponential rates with spatial dimension and propagation time. For these reasons, exact path integral calculations in general many-body systems appear to suffer from problems similar to those plaguing the traditional wavefunction approach. Nevertheless, the path integral provides the starting point for the formulation of numerical schemes that allow exact simulation of the dynamics in certain important situations, and the prospect for rigorous quantum-semiclassical treatments appears excellent.

The idea underlying the path integral formulation is the superposition principle. For a particle of mass m in one dimension, the amplitude to get from a point \mathbf{x}_0 to the point \mathbf{x}_f in time t is expressed in the path integral formulation as a sum of contributions from all conceivable paths that connect these points (92). The contribution of each path $\mathbf{x}(t)$ is proportional to a phase given by the action functional $S[\mathbf{x}(t)]$ along that path in units of Planck's constant \hbar :

$$\langle \mathbf{x}_f | e^{-iHt/\hbar} | \mathbf{x}_0 \rangle \propto \sum_{\substack{\text{all paths } \mathbf{x}(t) \\ \text{with } \mathbf{x}(0)=\mathbf{x}_0, \mathbf{x}(t)=\mathbf{x}_f}} e^{iS[\mathbf{x}(t)]/\hbar}. \tag{17}$$

Classical and nonclassical paths enter this expression with the same weight. In the classical limit $\hbar \rightarrow 0$, small variations of a path generally result in large changes in the phase S/\hbar . Because of destructive phase interference, the contributions of most paths sum to zero in this limit. Constructive interference results from paths whose actions are stationary, which are the classical trajectories. Using Equation 17 and the superposition principle for the evolution of a wavefunction, one can recover the conventional time-dependent Schrödinger equation (92).

Conversely, one can derive the path integral from the Schrödinger formulation of quantum mechanics. By slicing the total time t into N short time steps of length Δt and using the Trotter factorization of the short time-evolution operator, one arrives at the discretized path integral expression of the propagator (92):

$$\begin{aligned} \langle \mathbf{x}_f | e^{-iHt/\hbar} | \mathbf{x}_0 \rangle \approx & \left(\frac{m}{2\pi i\hbar\Delta t} \right)^{nN/2} \int_{-\infty}^{\infty} d\mathbf{x}_1 \cdots \int_{-\infty}^{\infty} d\mathbf{x}_{N-1} \\ & \times \exp \left(\frac{i}{\hbar} \frac{m}{2\Delta t} \sum_{k=1}^N |\mathbf{x}_k - \mathbf{x}_{k-1}|^2 - \frac{it}{2\hbar} [V(\mathbf{x}_k) + V(\mathbf{x}_{k-1})] \right), \end{aligned} \tag{18a}$$

which becomes an equality in the limit $N \rightarrow \infty$. Here, each realization of points $\mathbf{x}_0, \mathbf{x}_1, \dots, \mathbf{x}_{N-1}, \mathbf{x}_N \equiv \mathbf{x}_f$ defines a path that connects the initial and final point in the specified time. With finite values of the time step, the Feynman paths in Equation 18a are discretized. The exponent in that expression is easily recognized as the trapezoid rule discretization of the action in Feynman's ansatz, Equation 17.

In the continuous time limit, the propagator becomes a functional integral, for which Feynman employed the symbolic notation

$$\langle \mathbf{x}_f | e^{-iHt/\hbar} | \mathbf{x}_0 \rangle = \int \mathcal{D} \mathbf{x}(t') e^{iS(t')/\hbar}. \tag{18b}$$

Another alternative to the slicing employed in Equation 18a involves expansion of the paths in Fourier series (93).

The storage requirements of Equation 18 are minimal, but the large dimension of the integral involved appears to necessitate the use of Monte Carlo methods. However, as all paths enter the discretized path integral with the same weight, one needs to sample the entire volume of integration, and importance sampling does not offer an advantage. Most important, the rapid phase oscillation of the integrand results in enormous cancellation, which cannot be dealt with by Monte Carlo procedures (94).

The situation can be improved by constructing improved propagators that employ appropriate projection operators (94) or physically motivated reference systems (95) in the discretization of the path integral. These schemes lead to path integral expressions where the integrand is relatively localized and only mildly oscillatory with respect to each path integral variable. However, the effect of the residual oscillations (which are essential for reproducing quantum interference effects) is amplified in multidimensional space, leading to dramatic cancellation that renders Monte Carlo schemes inadequate for calculating the dynamics beyond a few time steps (94). Another attractive possibility is to bias the sampling near classical paths, where the phase is stationary and therefore phase cancellation is minimal (80, 96–98). This approach also suffers from the sign problem at longer times, as many stationary-phase paths begin to contribute with different phases that generally interfere destructively. In this sense, stationary-phase-based Monte Carlo path integral techniques cannot be less demanding than forward-time semi-classical propagation (discussed in the previous section), and usually the larger number of integration variables increases the numerical difficulty. In light of the analysis presented there, the use of a forward-backward representation in conjunction with stationary-phase sampling ideas may lead to a robust path integral scheme for simulating the quantum dynamics of large systems (99). Finally, an attractive idea that has been suggested is to rewrite the path integral in terms of the density of actions (100),

$$d(S) = \int \mathcal{D} \mathbf{x}(t') \delta(S - S[\mathbf{x}(t')]), \tag{19a}$$

which is directly amenable to computation by Monte Carlo methods. Using this concept, the propagator takes the form

$$\langle \mathbf{x}_f | e^{-iHt/\hbar} | \mathbf{x}_0 \rangle = \int dS d(S) e^{iS/\hbar}. \tag{19b}$$

The major advantage of this simple rearrangement is that the oscillatory component of the integrand is now one-dimensional and thus can be evaluated by quadrature. Preliminary application to one-dimensional models has been met with success, and the method appears promising. Note, however, that multidimensional calculations may require a high degree of accuracy in the density of actions, which may be difficult to attain by means of stochastic sampling.

Another possibility for extracting dynamical properties is via analytic continuation of imaginary time quantities (101–103), which are relatively straight forward to calculate. Analytic continuation methods are successful only if accurate data points are available. As a consequence, the presence of statistical error in the imaginary time data renders the process of analytic continuation to real time unstable in general. Moreover, the convergence radius of the propagator is not large in general, and this fact restricts the applicability of analytic continuation to fairly short times.

Maximum entropy image enhancement techniques (104) have been successfully applied to a variety of ill-conditioned problems, including the inversion of imaginary time quantities to obtain spectral properties. The maximum entropy method (105) finds the spectrum that corresponds to the largest number of ways of reproducing the data. By construction, the resulting spectrum has maximum entropy (in the information theoretic definition) subject to a number of constraints (106). Recent applications (107) indicate that the maximum entropy method can yield semiquantitative estimates of absorption spectra in solution and the corresponding real-time correlation functions up to moderate times. However, the method is not suitable for long time propagation.

An attractive idea is to infer useful dynamical information from statistical properties alone, avoiding the instability problems associated with real time calculations or inversion procedures. This is a fruitful strategy for estimating finite temperature reaction rates according to the centroid density formalism of Voth et al (108, 109). Following the work of Gillan (110, 111), the rate constant is expressed in terms of a constrained partition function, where the centroids

$$\mathbf{x}_c = (\hbar\beta)^{-1} \int_0^{\hbar\beta} \mathbf{x}(\tau) d\tau \quad 20.$$

of all cyclic quantum paths are forced to lie at the transition state. The centroid partition function

$$Z_c = \int \mathcal{D} \mathbf{x}(\tau) \delta(\mathbf{x}_c - \mathbf{x}_{\text{TS}}) e^{-\Phi[\mathbf{x}(\tau)]/\hbar}, \quad 21.$$

where Φ is the action in imaginary time and \mathbf{x}_{TS} denotes the location of the transition state, is then evaluated using the imaginary time path integral method (112). As real time dynamical effects are neglected, the centroid scheme is essentially a form of quantum mechanical transition-state theory. The method generally leads to a faithful estimation of the rate when the system-solvent coupling (the friction) is sufficiently strong. However, it fails to reproduce the so-called Kramers

turnover, i.e. the nonmonotonic variation of the rate observed in the activated regime for small friction values, and can significantly underestimate the rate in the deep tunneling regime (113). As classical transition-state theory can lead only to an overestimation of the reactive flux, it is clear that the latter effect has a quantum mechanical origin. A semiclassical analysis (114) has shown that enhancement of the rate at low temperature and weak friction is a consequence of coherence effects that survive even in a regime where the population dynamics are purely exponential.

Centroid density ideas have also been employed to formulate a centroid molecular dynamics (CMD) scheme in which the centroids evolve classically on a potential of mean force generated by integrating over quantum fluctuations of imaginary time paths (115, 116). In a recent application of the CMD method, Lobaugh & Voth (117) studied the quantum dynamics of an excess proton in liquid water. The potential interactions were described using a two-state empirical valence bond model for the H_5O_2^+ . The exchange of the proton between two water molecules was found to be an activationless quantum process, and the quantum infrared spectrum of the transferring proton was calculated. The authors concluded that quantum effects for the transferring proton are significant, qualitatively changing the radial distribution functions with respect to classical MD results.

To date, no stable fully quantum mechanical simulation methods are known that are applicable to arbitrary many-particle systems over long time periods. However, significant progress can be made by adopting the influence functional ideas pioneered by Feynman & Vernon (118). It is argued that rather than attempt to calculate the dynamics of a polyatomic system directly in full dimensionality, it is advantageous to partition the Hamiltonian into an observable, highly quantum mechanical subsystem (the reaction coordinate) and a bath of less interesting degrees of freedom, which are not probed directly. A generic Hamiltonian is then written as

$$H(s, p_s, \mathbf{x}, \mathbf{p}) \equiv H_s(s, p_s) + H_b(\mathbf{x}, \mathbf{p}) + V_{\text{int}}(s, \mathbf{x}). \quad 22.$$

Here s is the coordinate of the system of interest that is coupled to a generally nonlinear bath described by the coordinates x_j , which are denoted collectively by the vector \mathbf{x} . It is assumed that the system-bath interaction does not depend on momentum terms. The idea is to exploit linear response theory or semiclassical approximations to evaluate the influence of the environment on the observable system and to devise feasible schemes for evaluating the remaining sum over system paths.

Observables pertaining to the system of interest are conveniently expressed in terms of the reduced density matrix,

$$\langle s_f | \tilde{\rho}(t) | s_0 \rangle = \text{Tr}_b \langle s_f | e^{-iHt/\hbar} \rho(0) e^{iHt/\hbar} | s_0 \rangle, \quad 23.$$

where $\rho(0)$ is the initial density operator and the trace is with respect to the bath.

The reduced density matrix can be expressed as a double path integral in the form

$$\begin{aligned} \langle s_f | \tilde{\rho}(t) | s_0 \rangle &= \int ds' \int ds'' \int \mathcal{D}s_+ \int \mathcal{D}s_- e^{iS_0[s_+]/\hbar} \\ &\times \langle s' | \tilde{\rho}_0 | s'' \rangle e^{-iS_0[s_-]/\hbar} F[s_+, s_-]. \end{aligned} \quad 24.$$

Here S_0 is the action for the bare (or renormalized) system, $\tilde{\rho}_0$ is its initial density matrix, s_+ and s_- are forward and backward paths with endpoints (s', s_f) and (s'', s_0) , respectively, and F is the corresponding influence functional (118). Assuming that the system and bath are initially uncorrelated and that the bath is described by a canonical ensemble at a temperature $1/k_B\beta$, the influence functional is given by the expression

$$F[s_+, s_-] = Z^{-1} \text{Tr}_b(U[s_+] e^{-\beta H_b} U^{-1}[s_-]). \quad 25.$$

In the last equation, U is the time-evolution operator that corresponds to the (time-dependent) Hamiltonian $H_b + V_{\text{int}}$ along a given system path and Z is the partition function for the isolated environment. The assumption that the system and bath are initially uncorrelated is employed here only for the sake of simplifying the equations that follow; the general case of a bath that is equilibrated with respect to the system of interest can be treated via a straightforward (though slightly more cumbersome) extension of the procedures described below.

A special case of considerable significance is that of a low-dimensional non-linear system coupled to a dissipative bath of harmonic oscillators. The system-bath model can often provide a realistic description of the effects of common condensed-phase environments on the observable dynamics of the microscopic system of interest. A typical example is that of an impurity in a crystalline solid, where the harmonic bath arises naturally from the small-amplitude lattice vibrations. The harmonic picture is often relevant even in situations where the motion of individual solvent atoms is very anharmonic; in such cases, validity of the linear response approximation can lead to Gaussian behavior of appropriate effective modes by virtue of the central limit theorem (92, 114, 119, 120). The system-bath Hamiltonian under consideration can be written in the form (121)

$$H = \frac{p_s^2}{2m_0} + V_0(s) + \sum_j \left(\frac{p_j^2}{2m_j} + \frac{1}{2} m_j \omega_j^2 x_j^2 - c_j s x_j \right). \quad 26.$$

Here s denotes the coordinate of the quantum particle and x_j are the coordinates of the harmonic oscillator modes, which are linearly coupled to the system and which constitute the bath. For simplicity, the coupling functions are assumed linear in the system coordinate as well, although extension of the procedure that follows to a more general coupling form of the type $f_j(s)x_j$ is straightforward.

Accurate propagators for the Hamiltonian of Equation 26 are constructed by adding to the conventional kinetic energy reference (92) the potential along the

one-dimensional adiabatic path defined by the relations $x_j = c_j s / m_j \omega_j^2$ to construct a reference Hamiltonian:

$$H_0 = \frac{p_s^2}{2m_0} + V_0(s) - \sum_j \frac{c_j^2 s^2}{2m_j \omega_j^2}. \quad 27.$$

The reference propagator is calculated numerically (122, 123) in terms of the M lowest-energy eigenfunctions Φ_k and eigenvalues E_k of H_0 :

$$\langle s_b | e^{-iH_0 \Delta t / \hbar} | s_a \rangle = \sum_{k=1}^M \Phi_k(s_b) \Phi_k(s_a) e^{-iE_k \Delta t / \hbar}. \quad 28.$$

The remaining terms in the system-bath Hamiltonian correspond to linearly displaced harmonic oscillators, which enter the path integral in a Gaussian fashion. Following the procedure of Feynman & Vernon (118), these Gaussian variables are integrated out, leading to an influence functional that incorporates nonadiabatic corrections to the exact dynamics along the adiabatic path contained in the reference propagator. The resulting quasiadiabatic propagator path integral (QUAPI) expressions (95) converge with relatively large time steps.

In the discretized path integral language, the reduced density matrix takes the form

$$\begin{aligned} \tilde{\rho}(s'', s'; t) = & \int ds_0^+ \int ds_1^+ \cdots \int ds_{N-1}^+ \int ds_0^- \int ds_1^- \cdots \int ds_{N-1}^- \\ & \times \langle s'' | e^{-iH_0 \Delta t / \hbar} | s_{N-1}^+ \rangle \cdots \langle s_1^+ | e^{-iH_0 \Delta t / \hbar} | s_0^+ \rangle \\ & \times \langle s_0^+ | \tilde{\rho}(0) | s_0^- \rangle \langle s_0^- | e^{iH_0 \Delta t / \hbar} | s_1^- \rangle \cdots \langle s_{N-1}^- | e^{iH_0 \Delta t / \hbar} | s' \rangle \\ & \times F(s_0^+, s_1^+, \dots, s_{N-1}^+, s'', s_0^-, s_1^-, \dots, s_{N-1}^-, s'; \Delta t). \end{aligned} \quad 29.$$

Here $\{s_0^+, s_1^+, \dots\}$ and $\{s_0^-, s_1^-, \dots\}$ denote discretizations of the forward and backward path employed in the path integral representation of the forward and reverse time-evolution operators, respectively. The influence functional has the structure (118)

$$F = \exp \left(-\frac{1}{\hbar} \sum_{k=0}^N \sum_{k'=1}^k (s_k^+ - s_k^-) (\eta_{kk'} s_{k'}^+ - \eta_{kk'}^* s_{k'}^-) \right), \quad 30.$$

where the coefficients $\eta_{kk'}$ are discretized versions of the bath force autocorrelation function, which depends on the spectral features of the harmonic medium as well as the system-bath coupling coefficients. The influence functional contains interactions between path integral variables that may be separated by many time steps. This structure is reminiscent of the memory friction kernel in the classical generalized Langevin equation (124). Monte Carlo methods can be used successfully at short time intervals, for which the dimensionality of the integral in Equation 28 is not too high and phase cancellation is not extreme (125). However, the severity of the sign problem increases exponentially with the number of time

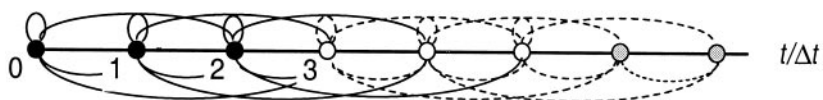


Figure 2 Diagrammatic representation of the path integral interactions in a case where the memory length is equal to three time steps. The *loops* indicate terms in the exponent of the influence functional. *Solid* and *dashed loops* indicate the decomposition of the path integral into an iterative procedure.

steps, and evaluation of the reduced density matrix by multidimensional Monte Carlo sampling is still problematic at intermediate-to-long time periods.

Fortunately, progress can be made in cases where the bath corresponds to a condensed medium. Because condensed-phase correlation functions decay within a finite interval, the effective length of nonlocal influence functional interactions is finite. Dropping negligible long-range correlations allows decomposition of the multidimensional path integral into a sequence of lower-dimensional operations (126, 127) (see Figure 2). Specifically, a reduced density functional (a multitime object) of path segments that span the pertinent memory length can be propagated forward in time via multiplication with an appropriate propagator functional (128). Restricting attention to those paths that enter the path integral with significant weight dramatically reduces the memory requirements of the method, and the filtered propagator functional (FPF) allows iterative evaluation of the path integral over very long time periods. In discrete time language, the reduced density functional becomes a vector and the propagator a matrix, such that the scheme reduces to matrix-vector multiplication. The essential difference from wavefunction propagation schemes is that the current case requires the use of larger matrices. Because the solvent memory length enters only as a convergence parameter, the scheme converges to the exact quantum mechanical result, and therefore the computed state populations approach the correct thermodynamic limit at long time periods. Golosov et al (129) recently showed that further correlations can also be neglected without significant loss of accuracy, leading to a convolution scheme with an integral equation kernel that drastically reduces the numerical effort required to simulate processes in long-memory solvents.

Using the FPF scheme, Sim & Makri (130) studied the dynamics of primary charge separation in bacterial photosynthetic reaction centers. By comparing the path integral simulation results to those from available time-resolved experiments, they concluded that the 3-ps electron transfer from the photoexcited special pair to the bacteriopheophytin proceeds via a two-step mechanism that utilizes the bacteriochlorophyll as a kinetic intermediate; however, as the second step of this sequential transfer is fast, the reduced bacteriochlorophyll state is depleted rapidly. The path integral time step employed in the simulations varied between 3 and 13 fs, such that the maximum propagation time in some of the calculations exceeded 5000 time steps.

The major limitation of the above real time path integral methodology is its restriction to processes occurring in harmonic media. To go beyond that assumption, one must resort to numerical methods for evaluating the influence functional from arbitrary polyatomic environments. Doing so at the level of full quantum mechanics does not appear feasible, as it amounts to calculating the dynamics of a many-body Hamiltonian. However, given the ensemble-averaged structure of the influence functional, the FBSD methodology described earlier is ideally suited. Using the coherent state representation (74), Makri & Thompson (87) arrived at the following forward-backward expression for a rigorous evaluation of the influence functional:

$$F[s_+, s_-] = Z_b^{-1} (2\pi\hbar)^{-1} \int d\mathbf{x}_0 \int d\mathbf{p}_0 D(\mathbf{x}_0, \mathbf{p}_0) \exp\left(\frac{i}{\hbar} S(\mathbf{x}_0, \mathbf{p}_0)\right) \times \langle G(\mathbf{x}_0, \mathbf{p}_0) | e^{-\beta H_b} | G(\mathbf{x}_f, \mathbf{p}_f) \rangle. \quad 31.$$

Here $\mathbf{x}_f, \mathbf{p}_f$ are the endpoints of a classical trajectory that starts with initial conditions $\mathbf{x}_0, \mathbf{p}_0$, evolves to time t under the combined forces as a result of the solvent and its interaction with the system along the given forward path s_+ , and subsequently returns to zero time, experiencing a force exerted on the solvent by the system along its backward path s_- . Finally, D is the Herman-Kluk prefactor in forward-backward time. Equation 31 is evaluated by a Monte Carlo procedure, which by virtue of the cancellation effected in the forward-backward action converges very well for system path pairs that lead to influence functionals appreciably different from zero (87). Numerical applications to a chain of 10 anharmonically coupled atoms modeling solvation shells in the radial direction around a chromophore (88) demonstrated that the method is robust and that calculations on moderate-size clusters are well within the power of current computer technology. Note also that the prospect of treating truly large systems appears good, as solvent atoms that are distant to the system of interest and thus weakly coupled to the latter make negligible contribution to the net action and therefore do not increase the difficulty of the calculation.

SUMMARY AND OUTLOOK

In recent years, time-dependent methods have advanced to the point that calculations on polyatomic systems are often feasible and reliable. Currently, the most widely used methods constitute a compromise between accuracy and feasibility. Typically, such schemes are based on one or more ad hoc approximations whose accuracy is hard to quantify. In general, dynamical approximations tend to perform well at short time periods, typically on the order of one period of the fastest degree of freedom treated explicitly, while often failing to describe long time events.

Thus, the development of economical methods capable of describing the dynamics beyond the first collision event remains a challenge.

The most rigorous of the available methods are computationally demanding, and their domain of applicability is not fully understood. It is therefore imperative to improve the efficiency of newly developed semiclassical and path integral methods in order to make them easily accessible. At the same time, an important goal is to use accurate methods for the purpose of testing less-expensive approximate schemes to establish their adequacy for treating complex chemical problems. These goals remain at the forefront of current research in theoretical quantum dynamics.

ACKNOWLEDGMENTS

This work has been supported by the David and Lucile Packard Foundation through a Packard Fellowship for Science and Engineering. I am grateful to Professor R Benny Gerber for many useful comments on the manuscript.

Visit the Annual Reviews home page at <http://www.AnnualReviews.org>

LITERATURE CITED

1. Dirac PA. 1930. *Proc. Cambridge Philos. Soc.* 26
2. McLachlan AD. 1964. *Mol. Phys.* 8: 39
3. Heller EJ. 1976. *J. Chem. Phys.* 64:63–73
4. Harris R. 1980. *J. Chem. Phys.* 72:1776
5. Gerber RB, Buch V, Ratner MA. 1982. *J. Chem. Phys.* 77:3022–30
6. Gerber RB, Ratner MA. 1988. *Adv. Chem. Phys.* 70:97–132
7. Billing GD. 1994. *Int. Rev. Phys. Chem.* 13:309
8. Rom AY, Neuhauser D, Gerber RB. 1998. *J. Chem. Phys.* 108:6084–92
9. Jungwirth P, Gerber RB. 1995. *J. Chem. Phys.* 102:6046
10. Wigner EJ. 1937. *Chem. Phys.* 5:720
11. Jungwirth P, Gerber RB. 1995. *J. Chem. Phys.* 102:8855
12. Jungwirth P, Fredj E, Gerber RB. 1996. *J. Chem. Phys.* 104:9332–39
13. Buch V, Gerber RB, Ratner MA. 1983. *Chem. Phys. Lett.* 101:44–48
14. Alimi R, Gerber RB, Hammerich AD, Kosloff R, Ratner MA. 1990. *J. Chem. Phys.* 93:6484–90
15. McCoy AB, Gerber RB. 1994. *J. Chem. Phys.* 101:1975–87
16. Fredj E, Gerber RB, Ratner MA. 1998. *J. Chem. Phys.* 109:4833
17. Makri N, Miller WH. 1987. *J. Chem. Phys.* 87:5781–87
18. Makri N. 1990. *Chem. Phys. Lett.* 169: 541–48
19. Meyer H-D, Manthe U, Cederbaum LS. 1990. *Chem. Phys. Lett.* 165:73–78
20. Manthe U, Meyer H-D, Cederbaum LS. 1992. *J. Chem. Phys.* 97:3199
21. Manthe U, Meyer H-D, Cederbaum LS. 1992. *J. Chem. Phys.* 97:9062–71
22. Worth GA, Meyer H-D, Cederbaum LS. 1996. *J. Chem. Phys.* 105:4412–26
23. Campos-Martinez J, Coalson RD. 1990. *J. Chem. Phys.* 93:4740–49
24. Campos-Martinez J, Coalson RD. 1993. *J. Chem. Phys.* 99:9629

25. Jackson B. 1988. *J. Chem. Phys.* 88:1383
26. Jackson B. 1986. *J. Chem. Phys.* 84:3535
27. Makri N. 1991. *J. Chem. Phys.* 94:4949–58
28. Mittelman MH. 1961. *Phys. Rev.* 122:499
29. Miller WH. 1974. *Adv. Chem. Phys.* 25:69
30. Wahnstrom G, Carmeli B, Metiu H. 1988. *J. Chem. Phys.* 88:2478–91
31. Haug K, Metiu H. 1992. *J. Chem. Phys.* 97:4781–91
32. Garcia-Vela A, Gerber RB. 1992. *J. Chem. Phys.* 97:7242–50
33. Ehrenfest P. 1927. *Z. Phys.* 45:455
34. Stock G. 1995. *J. Chem. Phys.* 103:1561–73
35. Wang H, Sun X, Miller WH. 1998. *J. Chem. Phys.* 108:9726–36
36. Blake NP, Metiu H. 1995. In *Femtosecond Chemistry*, ed. I. Manz, L. Wöste, 2:533–62. Weinheim: VCH
37. Bader JS, Berne BJ. 1994. *J. Chem. Phys.* 100:8359
38. Egorov SA, Berne BJ. 1997. *J. Chem. Phys.* 107:6050
39. Skinner JL. 1997. *J. Chem. Phys.* 107:8717
40. Billing GD. 1975. *Chem. Phys. Lett.* 30:391
41. Billing GD. 1975. *Chem. Phys.* 9:359
42. Meyer H-D, Müller WH. 1979. *J. Chem. Phys.* 70:3214–23
43. Tully JC. 1990. *J. Chem. Phys.* 93:1061–71
44. Tully JC, Preston RK. 1971. *J. Chem. Phys.* 55:562–72
45. Landau LD. 1932. *Phys. Z. Sowjetunion* 2:46
46. Zener C. 1932. *Proc. R. Soc. London Ser. A.* 137:696–703
47. Stueckelberg E. 1932. *Helv. Phys. Acta* 5:369
48. Space B, Coker DF. 1992. *J. Chem. Phys.* 96:652–63
49. Hammes-Schiffer S, Tully JC. 1994. *J. Chem. Phys.* 101:4657–67
50. Hammes-Schiffer S. 1996. *J. Chem. Phys.* 105:2236
51. Drukker K, Hammes-Schiffer S. 1997. *J. Chem. Phys.* 107:363
52. Pechukas P. 1969. *Phys. Rev.* 181:166–85
53. Coker DF, Xiao L. 1995. *J. Chem. Phys.* 102:496–510
54. Webster F, Rossky PJ, Friesner RA. 1991. *Comput. Phys. Commun.* 63:494–522
55. Webster FJ, Schnitker J, Friedrichs MS, Friesner RA, Rossky PJ. 1991. *Phys. Rev. Lett.* 66:3172–75
56. Long FH, Lu H, Eisinger KB. 1989. *Chem. Phys. Lett.* 160:464
57. Prezhdo OV, Rossky PJ. 1997. *J. Chem. Phys.* 107:825–34
58. Heller EJ. 1975. *J. Chem. Phys.* 62:1544–55
59. Heller EJ. 1981. *J. Chem. Phys.* 75:2923–30
60. Lee S-Y, Heller EJ. 1982. *J. Chem. Phys.* 76:3035–44
61. Henriksen NE, Heller EJ. 1989. *J. Chem. Phys.* 91:4700–13
62. Heller EJ. 1975. *Chem. Phys. Lett.* 34:321–25
63. Herrero CP, Ramirez R. 1995. *Phys. Rev. B* 51:16761–71
64. Martinez TJ, Ben-Nun M, Levine RD. 1997. *J. Phys. Chem.* 101:6389
65. Martinez TJ, Ben-Nun M, Levine RD. 1996. *J. Phys. Chem.* 100:7884
66. Ben-Nun M, Martinez TJ. 1998. *J. Chem. Phys.* 108:7244–57
67. Ben-Nun M, Martinez TJ, Levine RD. 1997. *Chem. Phys. Lett.* 270:319
68. Ben-Nun M, Molnar F, Lu H, Phillips JC, Martinez TJ, Schulten K. 1998. *Faraday Discuss. Chem. Soc.* 110:447
69. Van Vleck JH. 1928. *Proc. Natl. Acad. Sci. USA* 14:178
70. Miller WH. 1975. *Adv. Chem. Phys.* 30:77
71. Child MS. 1991. *Semiclassical Mechanics with Molecular Applications*. Oxford: Clarendon
72. Sepulveda MA, Tomsovic S, Heller EJ. 1992. *Phys. Rev. Lett.* 69:402–5
73. Miller WH. 1970. *J. Chem. Phys.* 53:3578–87
74. Herman MF, Kluk E. 1984. *Chem. Phys.* 91:27–34

75. Heller EJ. 1991. *J. Chem. Phys.* 94:2723
76. Ovchinnikov M, Apkarian VA. 1998. *J. Chem. Phys.* 108:2277–84
77. Ovchinnikov M, Apkarian VA. 1997. *J. Chem. Phys.* 105:10312
78. Walton AR, Manolopoulos DE. 1996. *Mol. Phys.* 84:961
79. Sepulveda MA, Grossman F. 1996. *Adv. Chem. Phys.* 96:191–304
80. Filinov VS. 1986. *Nucl. Phys. B* 271:717–25
81. Makri N, Miller WH. 1987. *Chem. Phys. Lett.* 139:10–14
82. Brewer ML, Hulme JS, Manolopoulos DE. 1997. *J. Chem. Phys.* 106:4832–39
83. Sun X, Miller WH. 1997. *J. Chem. Phys.* 106:916
84. Pollak E, Liao J-L. 1998. *J. Chem. Phys.* 108:2733–43
85. Sun X, Wang H, Miller WH. 1998. *J. Chem. Phys.* 109:7064–74
86. Sun X, Wang H, Miller WH. 1998. *J. Chem. Phys.* 109:4190–200
87. Makri N, Thompson K. 1998. *Chem. Phys. Lett.* 291:101–9
88. Thompson K, Makri N. 1999. *J. Chem. Phys.* 110:1343–53
89. Thompson K, Makri N. 1999. *Phys. Rev. E* 59:R4729–32
90. Miller WH. 1998. *Proc. Faraday Soc.* 110: 1–21
91. Feynman P. 1948. *Rev. Mod. Phys.* 20: 367–87
92. Feynman RP, Hibbs AR. 1965. *Quantum Mechanics and Path Integrals*. New York: McGraw-Hill
93. Doll JD, Freeman DL, Beck TL. 1990. *Adv. Chem. Phys.* 78:61
94. Makri N. 1991. *Comp. Phys. Commun.* 63:389–414
95. Makri N. 1995. *J. Math. Phys.* 36:2430–56
96. Makri N, Miller WH. 1988. *J. Chem. Phys.* 89:2170–77
97. Doll JD, Freeman DL, Gillan MJ. 1988. *Chem. Phys. Lett.* 143:277
98. Mak CH, Chandler D. 1990. *Phys. Rev. A* 41:5709–12
99. Makri N. Manuscript in preparation
100. Creswick RJ. 1995. *Mod. Phys. Lett. B* 9:693–99
101. Thirumalai D, Berne BJ. 1984. *J. Chem. Phys.* 81:2512–13
102. Thirumalai D, Berne BJ. 1991. *Comp. Phys. Commun.* 63:415–26
103. Behrman EC, Wolynes PG. 1985. *J. Chem. Phys.* 83:5863–69
104. Skilling J. 1989. In *Maximum Entropy and Bayesian Methods*, ed. J Skilling, Dordrecht, Netherlands: Kluwer
105. Jarrell M, Gubernatis JE. 1996. *Phys. Rep.* 269:133
106. Galliccio E, Berne BJ. 1994. *J. Chem. Phys.* 101:9909–18
107. Galliccio E, Berne BJ. 1996. *J. Chem. Phys.* 105:7064–78
108. Voth GA, Chandler D, Miller WH. 1989. *J. Chem. Phys.* 91:7749–60
109. Voth GA. 1996. *Adv. Chem. Phys.* 93: 135
110. Gillan MJ. 1987. *Phys. Rev. Lett.* 58:563–66
111. Gillan MJ. 1987. *J. Phys. C* 20:3621–41
112. Feynman RP. 1972. *Statistical Mechanics*. Redwood City, CA: Addison-Wesley
113. Topaler M, Makri N. 1994. *J. Chem. Phys.* 101:7500–19
114. Onuchic JN, Wolynes PG. 1988. *J. Phys. Chem.* 92:6495–503
115. Cao J, Voth GA. 1994. *J. Chem. Phys.* 101: 6157
116. Cao J, Voth GA. 1994. *J. Chem. Phys.* 100: 5106
117. Lobaugh J, Voth GA. 1996. *J. Chem. Phys.* 104:2056–69
118. Feynman RP, Vernon JFL. 1963. *Ann. Phys.* 24:118–73
119. Marcus RA. 1993. *Angew. Chem. Int. Ed. Engl.* 32:1111–21
120. Makri N. 1999. *J. Phys. Chem.* In press
121. Leggett AJ, Chakravarty S, Dorsey AT, Fisher MPA, Garg A, Zwerger M. 1987. *Rev. Mod. Phys.* 59:1–85
122. Makri N. 1992. *Chem. Phys. Lett.* 193: 435–44

-
123. Makri N. 1993. *J. Phys. Chem.* 97:2417–24
124. Kubo R, Toda M, Hashitsume N. 1991. *Statistical Physics*. Heidelberg: Springer-Verlag
125. Mak CH, Egger R. 1996. *Adv. Chem. Phys.* 93:39–76
126. Makri N, Makarov DE. 1995. *J. Chem. Phys.* 102:4600–10
127. Makri N, Makarov DE. 1995. *J. Chem. Phys.* 102:4611–18
128. Sim E, Makri N. 1997. *Comp. Phys. Commun.* 99:335–54
129. Golosov AA, Friesner RA, Pechukas P. 1999. *J. Chem. Phys.* 110:138–46
130. Sim E, Makri N. 1997. *J. Phys. Chem.* 101:5446–58